

# Experimental observation of two-dimensional Anderson localization with the atomic kicked rotor

Isam Manai,<sup>1</sup> Jean-François Clément,<sup>1</sup> Radu Chicireanu,<sup>1</sup> Clément Hainaut,<sup>1</sup>  
Jean Claude Garreau,<sup>1</sup> Pascal Sriftgiser,<sup>1</sup> and Dominique Delande<sup>2</sup>

<sup>1</sup>Univ. Lille, CNRS, UMR 8523 – PhLAM – Laboratoire de Physique des Lasers Atomes et Molécules, F-59000 Lille, France\*

<sup>2</sup>Laboratoire Kastler Brossel, UPMC, CNRS, ENS,  
Collège de France; 4 Place Jussieu, F-75005 Paris, France

Dimension 2 is expected to be the lower critical dimension for Anderson localization in a time-reversal-invariant disordered quantum system. Using an atomic quasiperiodic kicked rotor – equivalent to a two-dimensional Anderson-like model – we experimentally study Anderson localization in dimension 2 and we observe localized wavefunction dynamics. We also show that the localization length depends exponentially on the disorder strength and anisotropy and is in quantitative agreement with the predictions of the self-consistent theory for the 2D Anderson localization.

PACS numbers: 03.75.-b , 72.15.Rn, 05.45.Mt, 64.70.qj

The metal-insulator Anderson transition plays a central role in the study of quantum disordered systems. Using a tight-binding description of an electron in a lattice, Anderson [1] postulated in 1958 that the dominant effect of impurities in a crystal is to randomize the diagonal term of the Hamiltonian, and showed that this may lead to a localization of the wavefunction, in sharp contrast with the Bloch-wave solution for a perfect crystal. In a weakly disordered (3D) crystal, the eigenstates are delocalized, leading to a diffusive (metallic) transport, while strong disorder produces an insulator with localized eigenstates. From its original solid-state physics scope [1–4] this approach has been applied to a large class of systems in which waves propagate in disorder. This includes quantum-chaotic systems [5, 6] and electromagnetic radiation [7–9]. Important theoretical progress was obtained in ref. [10], which postulated that Anderson localization can be described by a one-parameter scaling law, leading to the prediction that, for  $d \leq 2$ , the dynamics is generically localized, even if the disorder is very weak. For  $d > 2$ , it predicted the existence of the Anderson transition between a diffusive dynamics at weak disorder and a localized dynamics at strong disorder.

There is no fully quantitative theory of Anderson localization, and analytic results are scarce. Supersymmetry techniques [11] allow derivation of expansions in powers of  $d - 2$  of the various quantities of interest, but reaching even  $d = 3$  is difficult. A useful, simplified theoretical approach is the so-called self-consistent theory of localization. In few words, it can be thought as a mean field theory where large fluctuations are neglected, but where weak localization corrections to transport, due to interference between time reversed multiply scattered paths, are included self-consistently. For spinless time-invariant systems, belonging to the orthogonal symmetry class [11], this approach correctly predicts the existence of the metal-insulator Anderson transition for  $d > 2$ , although it fails to predict the correct critical exponent.

For  $d = 1$ , it quantitatively predicts the localization length in a weak disorder. Other approaches lead to approximate values for the critical exponent not far from the numerical prediction [12].

Dimension  $d = 2$  – the lower critical dimension – is very special, the localization properties depending on the symmetry class. In the orthogonal symmetry class, the dynamics is always localized, but the localization length is predicted to scale *exponentially* with the inverse of the disorder strength, i.e.  $\xi \propto \ell \exp(\pi k \ell/2)$  [13] where  $k$  is the wavevector and  $\ell$  the mean-free path for propagation in the disordered medium. As discussed in the Supplemental Material [14], such an exponential dependence is a signature of the fact that  $d = 2$  is the lower critical dimension for Anderson localization. The 2D case has been previously studied experimentally in optical and ultracold atom systems [8, 15], but no quantitative indication of the exponential scaling has been demonstrated yet. In the present Letter, we use the well-known correspondence between the  $d$ -dimension Anderson model and the  $d$ -frequency quasiperiodic kicked rotor [6, 16, 17] to test experimentally these predictions.

The quasiperiodic kicked rotor (QPKR) [5, 6, 16–18] is a spatially one-dimensional system with an engineered time-dependence such that its dynamics is similar to the dynamics of a time-independent multidimensional system. The QPKR can be simply realized experimentally by exposing laser-cooled atoms (Cesium in the present work) to a delta-pulsed (kicked) laser standing wave of wavenumber  $k_L$  and time period  $T_1$ . The *amplitude* of the kicks is quasiperiodically time-modulated with a frequency  $\omega_2$ . The dynamics is effectively one-dimensional along the axis of the laser beam, as transverse directions are uncoupled. The corresponding Hamiltonian is:

$$H = \frac{p^2}{2} + K \cos x [1 + \varepsilon \cos(\omega_2 t)] \sum_{n=0}^{N-1} \delta(t - n), \quad (1)$$

where  $x$  is the particle position,  $p$  its momentum,  $K$  the

kick intensity and  $\varepsilon$  the amplitude of the modulation. We have chosen conveniently scaled variables such that distances along the  $x$  axis are measured in units of  $(2k_L)^{-1}$ , the particle's mass is unity and time is measured in units of the pulse period  $T_1$ . In the quantum case, a crucial parameter is  $\tilde{k} \equiv 4\hbar k_L^2 T_1/M$ , the reduced Planck constant.

For  $\varepsilon = 0$ , one obtains the periodic kicked rotor, which can be mapped onto a one-dimensional Anderson-like model [6], and displays “dynamical” localization [5, 19], that is, Anderson localization in momentum space instead of configuration space. For non-zero  $\varepsilon$ , the temporal dynamics of the QPKR is exactly that of a two-dimensional periodic kicked system [16, 17, 20], which itself can be mapped – provided  $2\pi/T_1, \omega_2$  and  $\tilde{k}$  are incommensurable numbers – onto a two-dimensional Anderson-like anisotropic-hopping model, where anisotropy is controlled by  $\varepsilon$  and the ratio of hopping to diagonal disorder is controlled by  $K/\tilde{k}$  [21].

The existence of a mapping of the kicked rotor onto an Anderson-like model has been used to experimentally observe 1D Anderson localization with atomic matter waves as early as 1995 [18]. The two-frequency modulation of the QPKR – which can be mapped on a 3D Anderson model [17, 20] – was used to experimentally observe 3D Anderson localization and the metal-insulator Anderson transition [22], measure accurately the critical exponent and demonstrate its universality [23].

The experimental study of the 2D case is more challenging than the 3D one, because the observation of the exponential behavior of the localization length  $p_{\text{loc}}$  requires  $p_{\text{loc}}$  to vary over about one order of magnitude. The localization time increasing with  $p_{\text{loc}}$ , this also requires the ability to preserve coherence over several hundreds kicks. This needed major evolutions of our experimental setup [24].

Experimentally, an atomic sample consisting of few million atoms is prepared in a thermal state (3.2  $\mu\text{K}$ ) whose momentum distribution is much narrower than the expected localization length. The atomic cloud is then “kicked” by a far-detuned ( $\Delta \approx 13$  GHz) pulsed standing wave (SW). Pulse duration is typically  $\tau = 300$  ns, while the typical pulse period  $T_1 = 27.778 \mu\text{s}$  corresponds to an effective Planck constant  $\tilde{k} = 2.89$ . According to Eq. (1), an adjustable amplitude modulation with  $\omega_2/2\pi = \sqrt{5}$  is superimposed to the kick sequence. In our previous experiments, to minimize coupling with gravity, the SW was horizontal. However, for 1000 kicks the atoms fall down by 3.8 mm, compared to the 1.5 mm SW waist, limiting the maximum number of kicks to 200. In order to overcome this limit we used in the present experiment a *vertical* SW, and the atoms fall freely between kicks. The new SW is formed by two beams that can be independently controlled, both in amplitude and phase, through a radio-frequency driving two acousto-optic modulators. This allows us to accurately cancel gravity effects, by imposing a linear frequency chirp to one arm of the SW

with respect to the other, so that the SW itself “falls” with acceleration  $g$ . A kicked rotor is thus realized in the free-falling reference frame. These technical improvements are discussed in more detail in the Supplemental Material [24]. At the end of the sequence, the velocity distribution is measured by a standard time-of-flight technique.

Figure 1(a) shows experimental momentum distributions  $\Pi(p)$  recorded after 0 to 1000 kicks for  $K = 5.34, \tilde{k} = 2.89, \varepsilon = 0.36$ . If the dynamics were classical, the momentum distribution would keep its initial Gaussian shape and the average kinetic energy increase linearly with time,  $E_{\text{kin}} = E_{\text{kin}}(t = 0) + Dt$ , where  $D$  is the classical diffusion constant in momentum space. In contrast, the experimental result displays a distribution which diffusively broadens at short times, but tends to freeze, i.e. to *localize* at long times. This clear-cut proof of localization is confirmed by the shape of the momentum distribution, shown in Fig. 1(b) after 200 kicks. It very clearly displays an exponential shape [25] (a straight line in the logarithmic plot)  $\exp(-|p|/p_{\text{loc}})/2p_{\text{loc}}$  characteristic of localization with a localization length  $p_{\text{loc}}$  [26]. Figure 1(c) shows the momentum distributions after 1000 kicks for  $K = 5.34, \tilde{k} = 2.89$  and increasing values of  $\varepsilon$ . It demonstrates that the localization length varies very rapidly with  $\varepsilon$ , indicating the evolution from a 1D localization at  $\varepsilon = 0$  to a truly 2D localization with a much longer localization length at  $\varepsilon = 0.6$ . In order to prevent trivial localization on KAM tori [27], we always used  $K > 4$ , ensuring that the classical dynamics is ergodic.

Instead of measuring the full momentum distribution, it is sufficient to measure the population  $\Pi_0(t)$  of the zero velocity class as

$$E_{\text{kin}} \propto \frac{1}{4\Pi_0^2(t)} \quad (2)$$

is proportional to  $\langle p^2 \rangle(t)$  (as the total number of atoms is constant) [28].

Figure 2 displays  $E_{\text{kin}}$  (at 1000 kicks) vs.  $\varepsilon$  for various values of  $K$  and  $\tilde{k}$ , showing that the exponential dependence in  $\varepsilon$  is a general feature, with a rate that decreases with  $\tilde{k}$  and increases with  $K$ . Note the overall  $E_{\text{kin}}$  dynamics of a factor of 60 (corresponding to a 8 fold increase in the localization length), a key feature of the present experiment.

The scaling theory of localization [10] predicts that dimension  $d = 2$  is the lower critical dimension for the Anderson transition. For a time-reversal invariant spinless system (thus belonging to the *orthogonal* universality class), all states are localized with an exponentially large localization length. For a usual 2D time-independent system, the relevant parameter is the dimensionless conductance at short scale, equal to the product  $k\ell$  of the wave vector by the mean free path, so that the logarithm of the localization length is proportional to  $k\ell$  [14].

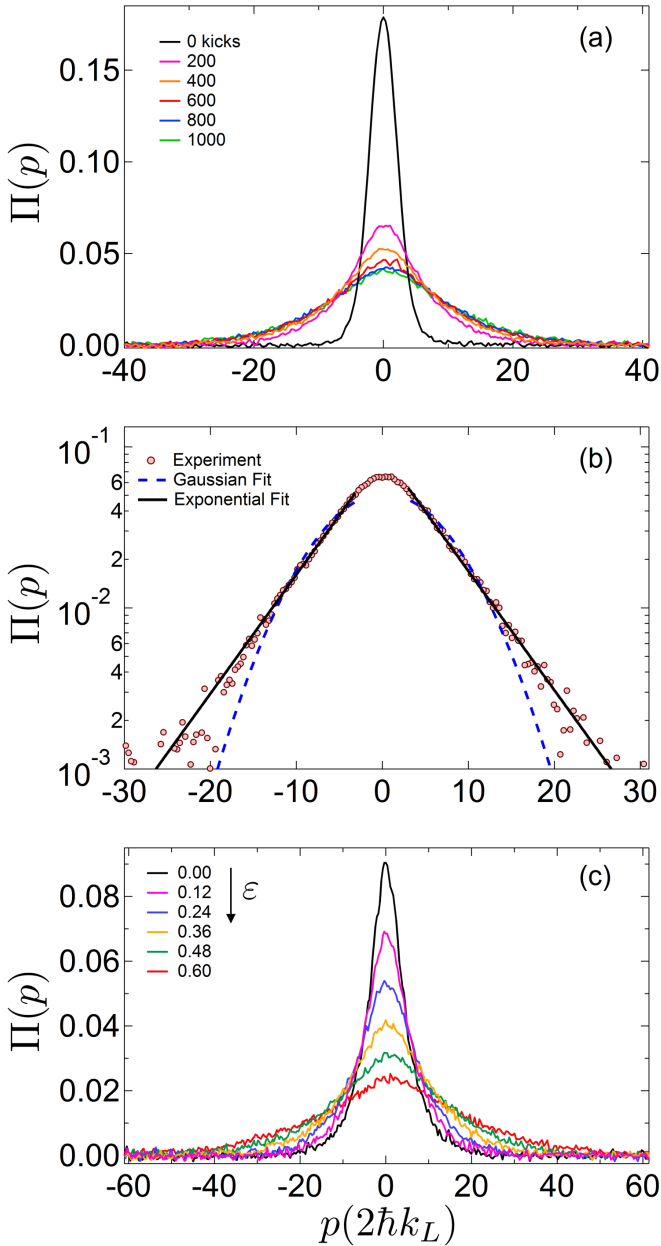


Figure 1. (Color online) Experimentally recorded momentum distributions for the kicked rotor exposed to a quasi-periodic driving, Eq. (1). (a)  $K = 5.34, \bar{k} = 2.89, \varepsilon = 0.36$ , 0 to 1000 kicks (step 200). The momentum distribution diffusively broadens at short times and freezes at longer times, proving the existence of 2D Anderson localization. Time increases from top to bottom curves. (b) Momentum distribution at 200 kicks in log scale, showing the exponential shape characteristic of localization. The circles are experimental points, the blue dashed line is a Gaussian fit and the black solid line an exponential fit for  $|p| > 3(2\hbar k_L)$ . (c) Localized momentum distributions after 1000 kicks, as a function of the anisotropy parameter  $\varepsilon$ , for  $K = 5.34, \bar{k} = 2.89$  as in (a) and (b). The modulation amplitude  $\varepsilon$  increases from top to bottom curves. The rapid increase of the localization length shows the evolution from the 1D localization at  $\varepsilon = 0$  to the truly 2D Anderson localization. Note the different horizontal scales in the various plots.

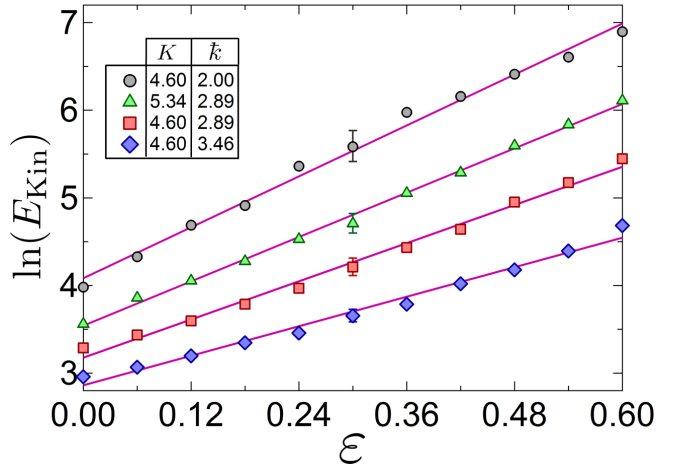


Figure 2. (Color online) Kinetic energy  $E_{\text{kin}}$  of the quasiperiodic kicked rotor vs. the modulation amplitude  $\varepsilon$ , for various values of the kicking strength  $K$  and effective Planck constant  $\bar{k}$ . The error bars indicate the typical experimental uncertainty. The four curves are straight lines in this logarithmic scale, with a slope that decreases with  $\bar{k}$  and increases with  $K$ .

The scaling theory cannot be directly transposed to the case of the kicked rotor for two reasons: i) There is no wavevector playing the role of  $k$ . Instead, one must consider the diffusion constant (in momentum space), which is, for a periodic kicked rotor, approximately equal to  $K^2/4$ . ii) The diffusion process for the 2D quasiperiodic kicked rotor is not isotropic. As shown in [29] and discussed in the Supplemental Material [14], the quasiperiodic kicked rotor can be mapped on a 2D Anderson-like model, whose dynamics at short time is indeed diffusive, but anisotropic. Along the “physical” direction (which coincides with the atom momentum component along the standing wave), the diffusion constant is – for small  $\varepsilon$  – almost equal to the one of the periodic kicked rotor,  $D_{11} \approx K^2/4$ ; along the other (virtual) direction, the diffusion constant is  $D_{22} \approx K^2\varepsilon^2/8$ , so that it vanishes in the limit  $\varepsilon \rightarrow 0$ , where one must recover the usual 1D periodic kicked rotor.

Altogether, the relevant parameter is the geometric average of the diffusion constant along the two directions  $\sqrt{D_{11}D_{22}} \propto \varepsilon K^2$ . The scaling theory predicts that the logarithm of the localization length should be proportional to  $\sqrt{D_{11}D_{22}}/\bar{k}^2$ . A similar prediction was made in [16] using a slightly different method.

The self-consistent theory of localization is an attempt towards more quantitative predictions, based on the same ideas as the scaling theory. It has been successfully used to predict properties of the Anderson transition [30, 31], and was transposed to the periodic kicked rotor in [19, 32] and to the quasiperiodic kicked rotor with two additional driving frequencies in [33]. It consists in computing perturbatively the weak localization correction to the

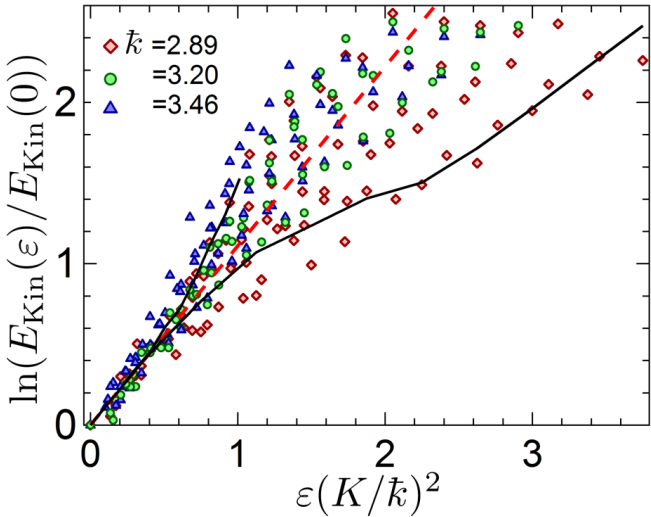


Figure 3. (Color online) Increase in the kinetic energy at  $t = 1000$  ( $\propto p_{\text{loc}}^2$ ) of the quasiperiodic kicked rotor with respect to the purely one-dimensional situation  $\varepsilon = 0$  vs. the scaling parameter  $\varepsilon(K/k)^2$ . The cloud of experimental points – collected at various values of  $K$ ,  $\varepsilon$  and  $k$  – is distributed around an average linear dependence in this semi-logarithmic plot, which shows the exponential dependence of the localization length, characteristic of 2D Anderson localization. The red dashed line is the prediction of Eq. (3). The spread is due in part to experimental imperfections (at large  $\varepsilon(K/k)^2$ , the localization time is not much shorter than the duration of the experiment) and in part to fundamental reasons: The linear dependence on  $\varepsilon K^2/k^2$  in the argument of the exponential, Eq. (3), is valid only at small  $\varepsilon$ , and the formula assumes that the classical diffusion constant is proportional to  $K^2$ , while the actual diffusion constant has oscillatory corrections. The black curves are numerical simulations corresponding to the two “extreme” values of  $K/k = 1.3, k = 3.46$  (higher curve) and  $K/k = 2.5, k = 2.89$  (lower curve); they display the same spreading phenomenon.

(anisotropic) diffusion constant and to extrapolate to the strong localization regime. It however depends on the cut-offs used. For our quasiperiodic kicked rotor [14] it confirms the prediction of the scaling theory, namely:

$$p_{\text{loc}} = \frac{K^2}{4k} \exp\left(\frac{\alpha \varepsilon K^2}{k^2}\right) \quad (3)$$

where  $\alpha$  is a number of the order unity, which may however depend smoothly on the parameters. In the limit  $\varepsilon \rightarrow 0$ , it is  $\alpha = \pi/\sqrt{32}$ .

In Fig. 3, we display the results of 275 measurements, corresponding to 12 values of the ratio  $K/k \in [1.3, 2.5]$ , with  $K \in [4.33, 7.26]$  and  $k = \{2.89, 3.2, 3.46\}$ , and to  $\varepsilon$  values from 0 to 0.6 (step 0.06). Dividing  $E_{\text{kin}}(\varepsilon)$  by  $E_{\text{kin}}(\varepsilon = 0)$  makes it possible to probe the exponential term in Eq. (3). The exponential dependence (straight line in logarithmic scale) is visible for  $\varepsilon \lesssim 1$ , materialized by the red dashed line, corresponding to the prediction

$\alpha = \pi/\sqrt{32}$  of the self-consistent theory. Despite the spreading of the experimental results around the average trend, the overall agreement is rather good. This proves the exponential dependence of the localization length in 2D, and thus that  $d = 2$  is the lower critical dimension for the metal-insulator Anderson transition. Some deviations are nevertheless visible. They arise from different phenomena: First, for large  $\varepsilon$ , the localization time can be only slightly shorter than the duration of the experiment (1000 kicks), meaning that the measured momentum distribution is not the asymptotic one for infinite time and underestimates the eventual saturation of  $E_{\text{kin}}$  at long time. This explains why the experimental points at large  $\varepsilon$  tend to lie below the theoretical prediction. This is confirmed by numerical calculations in the experimental conditions for the largest value of  $K/k = 2.5$  (longest localization time), see the solid lower curve in Fig. 3. A second, more fundamental, phenomenon is that Eq. (3) assumes that the classical diffusion constant is simply  $K^2/4$ , which is valid only for  $K \gg 1$ , whereas oscillatory corrections at moderate  $K$  are known to exist for the 1D kicked rotor [34] and to persist even for the 3D QPKR [29]. This dependence is thus not eliminated by the normalization to  $E_{\text{kin}}(\varepsilon = 0)$ . This explains a significant part of the spreading of the data. Finally, Eq. (3) is expected to be valid in the  $\varepsilon \rightarrow 0$  limit, see Supplemental Material [14]. At larger  $\varepsilon$  values, higher order terms must come into play and are responsible for significant deviations. This is visible in Fig. 3, where both experimental (points) and numerical (solid lines) data are well predicted at small  $\varepsilon K^2/k^2$ , but are more widely spread as  $\varepsilon K^2/k^2$  increases. A thorough analysis of all these deviations is beyond the scope of this Letter.

To summarize, we presented the first experimental evidence of two-dimensional Anderson localization with atomic matter waves. We studied the variation of the localization length with the system parameters and showed that it displays an exponential dependence characteristic of time-reversal spinless systems. To the best of our knowledge, such an experimental evidence has not been observed previously. It demonstrates experimentally that  $d = 2$  is the lower critical dimension of the Anderson transition. The observed localization length varies as predicted by the scaling and the self-consistent theories of localization.

The authors acknowledge M. Lopez for his help in the early stages of this experiment. DD thanks N. Cherroret, S. Ghosh and C. Tian for discussions on the self-consistent theory of localization. This work was supported by Agence Nationale de la Recherche (Grants LAKRIDI No. ANR-11-BS04-0003 and K-BEC No. ANR-13-BS04-0001-01), the Labex CEMPI (Grant No. ANR-11-LABX-0007-01), and “Fonds Européen de Développement Economique Régional” through the “Programme Investissements d’Avenir”. This work was granted access to the HPC resources of TGCC under

the allocation 2015-057083 made by GENCI (“Grand Equipement National de Calcul Intensif”) and to the HPC resources of The Institute for Scientific Computing and Simulation financed by Region Ile de France and the project Equip@Meso (Grant No. ANR-10-EQPX-29-01).

## Appendix: Supplemental Material

The following Supplemental Material discusses:

- I. The main improvements in our experimental setup allowing the 2D Anderson localization to be observed.
- II. The mapping of the quasiperiodic kicked rotor onto a 2D Anderson model, indicating the essentials of this mapping and its peculiarities relevant for the present work.
- III. The classical diffusion in the 2-frequency quasiperiodic kicked rotor.
- IV. A schematic derivation of the localization length, indicating the essential steps of the calculation in the case of the quasiperiodic kicked rotor with 2 incommensurate frequencies and the origin of the exponential dependence on the anisotropy.

### 1. Setup improvements

In our previous experiments, in order to minimize coupling with gravity, the standing wave (SW) was horizontal, see Fig. 4a. This geometry has several drawbacks. For 1000 kicks, the atoms would fall of 3.8 mm, to be compared to the 1.5 mm of the SW waist. Moreover, the SW was built by retro-reflecting the incoming beam, which leads to a  $\sim 1$  m optical path difference between the two beams overlapping on the atomic cloud region, a source of phase noise detrimental to dynamical localization. These restrictions limited the kick number to less than 200 in our previous experiments. In order to overcome this limit, we built a new SW system with several improvements, as shown in Fig. 4b. The SW is now vertical, and, between kicks, the atoms fall freely. The intensity inhomogeneity in the transverse direction was also reduced. The SW is now formed by two independent beams, which has many advantages, as each arm can be independently controlled, both in amplitude and phase through the radio-frequency wave that drives the acousto-optic modulators. This allows us to accurately cancel gravity effects, by imposing a linear frequency chirp to one of the arms with respect to the other, so that the SW itself “falls” with acceleration  $g$ . A kicked rotor is thus realized in the free-falling reference frame. Finally, the SW phase noise induced by the laser linewidth

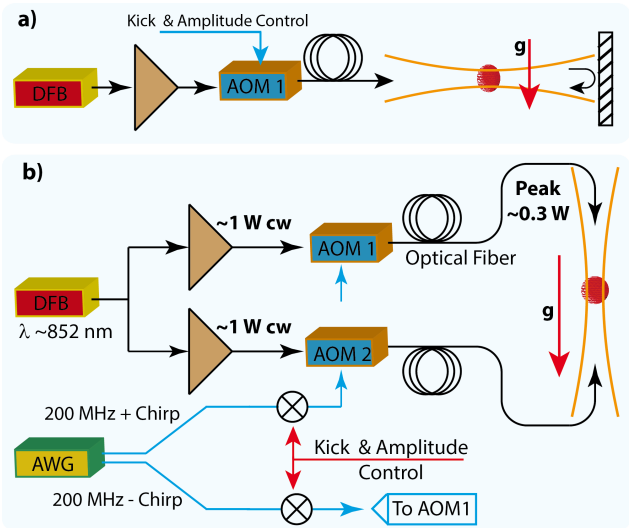


Figure 4. Evolution of the experimental setup. a) Horizontal standing wave setup used in former experiments. The kicks are controlled by a single acousto-optic modulator (AOM), and the standing wave is built by retro-reflecting the incoming laser beam. b) Schematic view of the new vertical setup used in the present work. A Distributed Feedback Laser Diode (DFB) seeds two optical amplifiers. The kick-sequence temporal modulation is produced by an arbitrary wave generator (AWG). In addition to the pulsed sequence, a linear chirp is added so that the standing wave “falls” with acceleration  $g$ , simultaneously with the atomic cloud.

is minimized by accurately balancing the optical paths of the arms to better than 1 cm. This is performed by directly minimizing the kinetic energy dispersion at 1000 kicks with a 1D kicked rotor.

### 2. Mapping of the quasiperiodic kicked rotor onto a 2D Anderson model

The mapping of the quasiperiodic kicked rotor (QPKR) onto a 2D Anderson model has been described in [16, 17, 20]. Because it is useful to derive an approximate expression for the localization length, we summarize here the basics of the calculation.

The starting point is the following Hamiltonian:

$$\mathcal{H} = \frac{p_1^2}{2} + \omega_2 p_2 + K \cos x_1 [1 + \varepsilon \cos x_2] \sum_n \delta(t-n) \quad (A.1)$$

which describes a *periodically kicked*, two-dimensional “rotor”; we use here quotation marks around “rotor” because of the unusual form of the kinetic energy along the direction 2, linear instead of quadratic. It is a matter of algebra [20] to show that the temporal evolution of an initial state initially localized at  $x_2 = \phi_2$ , but with arbitrary wave-function along  $x_1$ :

$$\Psi(x_1, x_2, t = 0) \equiv \Xi(x_1, t = 0) \delta(x_2 - \phi_2) \quad (A.2)$$

leads to the state:

$$\Psi(x_1, x_2, t) = \Xi(x_1, t) \delta(x_2 - \phi_2 - \omega_2 t), \quad (\text{A.3})$$

where the wavefunction  $\Xi(x_1, t)$  *exactly* obeys the time-dependent Schrödinger equation of the quasiperiodic kicked rotor:

$$H = \frac{p_1^2}{2} + K \cos x_1 [1 + \varepsilon \cos(\omega_2 t + \phi_2)] \sum_n \delta(t - n). \quad (\text{A.4})$$

Thus, the evolution of the quasiperiodic kicked rotor can be thought of as the evolution of a 2D periodic “rotor”, with a peculiar initial state perfectly localized in the  $x_2$  direction and thus completely delocalized in the conjugate  $p_2$  direction.

The Hamiltonian Eq. (A.1) being time-periodic, one can use the Floquet theorem and look at its Floquet eigenstates. Let  $|\phi\rangle$  denote an eigenstate of the evolution operator over one period with eigenvalue  $\exp(-iE/\hbar)$ , and consider the state  $|\chi\rangle = (1 + iW)^{-1}|\phi\rangle$  where  $W(x_1, x_2) \equiv \tan[K \cos x_1 (1 + \varepsilon \cos x_2) / 2\hbar]$ . The Hamiltonian being periodic in  $x_1$  and  $x_2$  (we take periodic boundary conditions),  $|\chi\rangle$  can be expanded on the basis of plane waves  $|m_1, m_2\rangle$  – eigenstates of the momentum operators in both directions with eigenvalues  $m_1\hbar$  and  $m_2\hbar$ :  $|\chi\rangle = \sum_{m_1, m_2} \chi_{m_1, m_2} |m_1, m_2\rangle$ . It is again a matter of algebra [6, 17] to show that the coefficients  $\chi_{m_1, m_2}$  obey the following equation:

$$\epsilon_{m_1, m_2} \chi_{m_1, m_2} + \sum_{r_1, r_2 \neq 0} W_{r_1, r_2} \chi_{m_1 + r_1, m_2 + r_2} = 0, \quad (\text{A.5})$$

where  $\epsilon_{m_1, m_2}$  is given by:

$$\epsilon_{m_1, m_2} = \tan \left\{ \frac{1}{2} \left[ \left( \hbar \frac{m_1^2}{2} + \omega_2 m_2 \right) - \frac{E}{\hbar} \right] \right\} \quad (\text{A.6})$$

and the  $W_{r_1, r_2}$  are the two-fold Fourier components of the doubly-periodic function  $W$ .

Equation (A.5) can be interpreted as the eigenvalue equation for a Anderson-like model on a 2D lattice with sites labeled  $(m_1, m_2)$ , with hopping described by  $W_{r_1, r_2}$  and on-site energies  $\epsilon_{m_1, m_2}$ . There are however four differences with respect to a usual Anderson model:

- The hopping matrix elements  $W_{r_1, r_2}$  are not limited to nearest neighbors. They do however decrease fast enough at large  $(r_1, r_2)$  so that this difference does not change the qualitative behavior (i.e. localization).
- The on-site energies  $\epsilon_{m_1, m_2}$  are not random, but rather a deterministic pseudo-random sequence. Provided  $\pi, \hbar, \omega_2$  are incommensurate, the sequence has no periodicity and localization properties similar to those of a truly random model are expected (and observed numerically).

- The hopping is anisotropic, governed by the  $K/\hbar$  coefficient along direction 1 and by the  $\varepsilon K/\hbar$  coefficient along direction 2. For  $\varepsilon = 0$ , the 2D system appears as a series of chains along direction 1, which are uncoupled along direction 2, and a 1D Anderson model is recovered.

- Floquet quasi-eigenstates with different quasi-energies  $E$  are associated with the same energy 0 in Eq. (A.5), but with different realizations of the disorder, Eq. (A.6), all having the same statistical properties. This is why, for given values of parameters  $\hbar, K, \varepsilon$ , all quasi-eigenstates have the same localization length [14].

In order to understand localization properties of the quasiperiodic kicked rotor, it is thus sufficient to study transport and localization on the equivalent anisotropic Anderson-like 2D model Eq. (A.1).

### 3. Classical diffusion

It is well known that the classical dynamics of the periodic kicked rotor is described by the Standard Map [27]. A similar map can be constructed for the quasiperiodic kicked rotor. The classical evolution over one period of the Hamiltonian Eq. (A.4) is given by the following map:

$$\begin{aligned} p_{1n+1} &= p_{1n} + K \sin x_{1n} (1 + \varepsilon \cos x_{2n}), \\ p_{2n+1} &= p_{2n} + K \varepsilon \cos x_{1n} \sin x_{2n}, \\ x_{1n+1} &= x_{1n} + p_{1n+1}, \\ x_{2n+1} &= x_{2n} + \omega_2, \end{aligned}$$

where  $y_n = y(t = n + \epsilon)$ ,  $y = x_i, p_i$  ( $i = 1, 2$ ). If  $K$  is sufficiently large, the classical dynamics is almost fully chaotic [29]. For the 1D problem ( $\varepsilon = 0$ ), this takes place for  $K \gtrsim 6$ . For the 2D problem (non vanishingly small  $\varepsilon$ ), we found an almost fully chaotic dynamics for  $K \gtrsim 4$ , and this is why we did not perform any experiment below this value. In the chaotic regime, the kicks in momentum have a pseudo-random sign (depending on  $x_1$  and  $x_2$ ), making the dynamics in momentum space appear as a pseudo-random walk, i.e. a chaotic diffusive process at long time. Note however that the diffusion is anisotropic because kicks along  $p_2$  are typically smaller than kicks along  $p_1$  by a factor  $\varepsilon$ . In the limit of large  $K$  it is easy to evaluate the diffusion tensor, defined as

$$D_{ij} = \lim_{t \rightarrow +\infty} \frac{\langle p_i p_j \rangle}{t} \quad (\text{A.7})$$

by assuming that positions of consecutive kicks are uniform uncorrelated variables (see [29] for the essentially identical calculation in 3D). It is diagonal in the (1,2)

directions with:

$$\begin{aligned} D_{11} &\approx (K^2/4)(1 + \varepsilon^2/2), \\ D_{22} &\approx K^2 \varepsilon^2/8, \\ D_{i \neq j} &\approx 0. \end{aligned} \quad (\text{A.8})$$

Numerical simulations of the classical dynamics [29] fully confirm that the classical dynamics is an anisotropic diffusion; however, at not too large  $K$ , correlations between successive kicks are responsible for oscillatory corrections to the diffusion constant of the order of few ten percents.

#### 4. Localization length

The calculation of the localization length turns out to a bit tricky in 2D. It has been discussed in the literature mainly in the context of electrons in disordered potentials [35, 36]. The calculation for the quasiperiodic rotor follows the same lines. We sketch here only the general method, comparing the key steps with the case of electrons in disordered potentials.

The starting point is to take into account the weak localization effect due to closed loops in the system. In the weak scattering regime, where this correction is small, it takes the following form for electrons (or massive particles) in disordered potentials:

$$\frac{\mathcal{D}}{D} = 1 - \frac{1}{\pi\rho} \int \frac{1}{(2\pi)^2} \frac{d\mathbf{q}}{Dq^2} \quad (\text{A.9})$$

where  $D$  is the classical (Boltzmann) diffusion constant and  $\mathcal{D}$  the quantum modified one. The term after 1 in the right-hand side is the weak localization correction. It depends on the density of states  $\rho$  and involves a two-dimensional integral over the vector  $\mathbf{q}$  which is a momentum, conjugate of position. The integrand is nothing but the classical diffusive kernel (at zero frequency, hence infinite time). Formally, the integral diverges both for small and large  $q$ , so that appropriate cut-offs must be set. The natural short distance (large  $q$ ) cut-off is the mean free path  $\ell$  (at shorter scale, the dynamics is not diffusive). The short  $q$  cut-off can be taken proportional to  $1/L$ , where  $L$  is the size of the system. One then obtains a size-dependent diffusion constant  $\mathcal{D}(L)$ . Taking for the density of states in 2D its disorder-free value  $1/2\pi$  (we take the mass of the particle and  $\hbar$  as unity), one obtains:

$$\frac{\mathcal{D}(L)}{D} = 1 - \frac{2}{\pi k\ell} \ln\left(\frac{L}{\ell}\right) \quad (\text{A.10})$$

where  $k$  is the wavevector of the particle. In these units, the classical diffusion constant is  $D = k\ell/2$ . The logarithmic dependence in  $L$  is a crucial ingredient, as we will see below. It is intimately related to the low- $q$  divergence of the integral.

Equation (A.10) shows that the diffusion constant decreases with the system size. Of course, this cannot be

correct for arbitrary large size, as the correction is computed assuming it is small. This ceases to be true when the right hand side term in Eq. (A.10) vanishes. This gives an order of magnitude of the size at which the diffusion constant vanishes, that is the localization length. One then gets

$$\xi = \ell \exp\left(\frac{\pi k\ell}{2}\right). \quad (\text{A.11})$$

Of course, this is only a very approximate expression. The self-consistent theory of localization [35, 36] is an attempt to be a bit more quantitative. It predicts essentially the same exponential dependence for the localization length.

For the periodic kicked rotor, the weak localization corrections have been computed in [19]. These results have been extended to the quasiperiodic rotor in [33, 37]. There are essentially two modifications:

- The term depending on the density of states (which is meaningless for a time-periodic system where the density of states of the Floquet Hamiltonian is infinite)  $1/\pi\rho$  must be replaced by  $2k^2$ .
- Because the classical dynamics is an anisotropic diffusion, the diffusive kernel is now  $(D_{11}q_1^2 + D_{22}q_2^2)^{-1}$ . When performing the integral over  $\mathbf{q}$ , it is not entirely clear how to choose the cut-offs. The simplest choice is to take the large  $q_1$  and  $q_2$  cut-offs scaling like the (anisotropic) mean free paths, i.e. respectively proportional to  $1/\sqrt{D_{11}}$  and  $1/\sqrt{D_{22}}$ . This is however arbitrary and questionable. It is important to understand that the choice of different cut-offs will affect the prefactors, but not the key point, namely the logarithmic dependence of the integral on the system size.

With this simple choice of cut-offs, the weak localization correction reads:

$$\frac{\mathcal{D}_{11}(L)}{D_{11}} = \frac{\mathcal{D}_{22}(L)}{D_{22}} = 1 - \frac{k^2}{\pi\sqrt{D_{11}D_{22}}} \ln\left(\frac{L}{l}\right) \quad (\text{A.12})$$

where  $l$  is a yet unspecified short scale cut-off.

With the same reasoning as the one for electrons, one obtains the approximate expression for the localization length (in momentum space for the kicked rotor):

$$p_{\text{loc}} = l \exp\left(\frac{\pi\sqrt{D_{11}D_{22}}}{k^2}\right). \quad (\text{A.13})$$

In the  $\varepsilon \rightarrow 0$  limit, one must recover the localization length of the periodic kicked rotor, which fixes  $l = K^2/4k$ . By inserting the values of the diffusion constants, Eqs. (A.8) into Eq. (A.13), we finally obtain:

$$p_{\text{loc}} = \frac{K^2}{4k} \exp\left(\frac{\pi\varepsilon K^2}{\sqrt{32k^2}}\right). \quad (\text{A.14})$$

Because of the questionable assumptions on the cut-offs, it might well be that the coefficient  $\pi/\sqrt{32}$  is not exact and requires some correction. This is a difficult question left for further investigation. We just emphasize that the exponential behavior of the localization length with the scaling parameter  $\varepsilon K^2/k^2$  comes from the prefactors in the integral over  $\mathbf{q}$  and from the logarithmic singularity of the integral. It is thus a very robust phenomenon, unlikely to be affected by the shortcomings of the self-consistent theory of localization. Ultimately, the *experimentally observed* exponential dependence of the localization length *proves* that the weak localization correction is logarithmic with the system size. This, in turn, implies that dimension  $d = 2$  is the lowest critical dimension of the Anderson transition. Indeed, a modification of the dimension would introduce an extra  $q^{d-2}$  factor in the integral, i.e. would change the logarithm dependence in  $L$  in Eq. (A.12) to an algebraic one, incompatible with the exponential behavior of the localization length.

---

\* [www.phlam.univ-lille1.fr/atfr/cq](http://www.phlam.univ-lille1.fr/atfr/cq)

- [1] P. W. Anderson, “Absence of Diffusion in Certain Random Lattices,” *Phys. Rev.* **109**, 1492–1505 (1958).
- [2] D. M. Basko, I. L. Aleiner, and B. L. Altshuler, “Metal-insulator transition in a weakly interacting many-electron system with localized single-particle states,” *Ann. Phys.* **321**, 1126–1205 (2006).
- [3] B. Kramer and A. Mackinnon, “Localization: theory and experiment,” *Rep. Prog. Phys.* **56**, 1469–1564 (1993).
- [4] D. J. Thouless, “Electrons in disordered systems and the theory of localization,” *Phys. Rep.* **13**, 93–142 (1974).
- [5] G. Casati, B. V. Chirikov, J. Ford, and F. M. Izrailev, “Stochastic behavior of a quantum pendulum under periodic perturbation,” in *Stochastic Behavior in Classical and Quantum Systems*, Vol. 93, edited by G. Casati and J. Ford (Springer-Verlag, Berlin, Germany, 1979) pp. 334–352.
- [6] D. R. Grempel, R. E. Prange, and S. Fishman, “Quantum dynamics of a nonintegrable system,” *Phys. Rev. A* **29**, 1639–1647 (1984).
- [7] M. Störzer, P. Gross, C. M. Aegerter, and G. Maret, “Observation of the Critical Regime Near Anderson Localization of Light,” *Phys. Rev. Lett.* **96**, 063904 (2006).
- [8] T. Schwartz, G. Bartal, S. Fishman, and M. Segev, “Transport and Anderson localization in disordered two-dimensional photonic lattices,” *Nature (London)* **446**, 52–55 (2015).
- [9] C. Dembowski, H. D. Gräf, R. Hofferbert, H. Rehfeld, A. Richter, and T. Weiland, “Anderson localization in a string of microwave cavities,” *Phys. Rev. E* **60**, 3942–3948 (1999).
- [10] E. Abrahams, P. W. Anderson, D. C. Licciardello, and T. V. Ramakrishnan, “Scaling Theory of Localization: Absence of Quantum Diffusion in Two Dimensions,” *Phys. Rev. Lett.* **42**, 673–676 (1979).
- [11] F. Evers and A. D. Mirlin, “Anderson transitions,” *Rev. Mod. Phys.* **80**, 1355–1417 (2008).
- [12] A. M. García-García, “Semiclassical Theory of the Anderson Transition,” *Phys. Rev. Lett.* **100**, 076404 (2008).
- [13] R. C. Kuhn, O. Sigwarth, C. Miniatura, D. Delande, and C. A. Müller, “Coherent matter wave transport in speckle potentials,” *New J. Phys.* **9**, 161 (2007).
- [14] See Supplemental Material at [URL will be inserted by publisher], which includes Refs. [35–37], for details on the scaling theory and on the self-consistent theory of 2D localization in the kicked rotor.
- [15] M. Robert-de-Saint-Vincent, J.-P. Brantut, B. Allard, T. Plisson, L. Pezzé, L. Sanchez-Palencia, A. Aspect, T. Bourdel, and P. Bouyer, “Anisotropic 2D Diffusive Expansion of Ultracold Atoms in a Disordered Potential,” *Phys. Rev. Lett.* **104**, 220602 (2010).
- [16] D. L. Shepelyansky, “Localization of diffusive excitation in multi-level systems,” *Physica D* **28**, 103–114 (1987).
- [17] G. Casati, I. Guarneri, and D. L. Shepelyansky, “Anderson Transition in a One-Dimensional System with Three Incommensurate Frequencies,” *Phys. Rev. Lett.* **62**, 345–348 (1989).
- [18] F. L. Moore, J. C. Robinson, C. F. Bharucha, B. Sundaram, and M. G. Raizen, “Atom Optics Realization of the Quantum  $\delta$ -Kicked Rotor,” *Phys. Rev. Lett.* **75**, 4598–4601 (1995).
- [19] A. Altland, “Diagrammatic approach to Anderson localization in the quantum kicked rotator,” *Phys. Rev. Lett.* **71**, 69–72 (1993).
- [20] G. Lemarié, J. Chabé, P. Sriftgiser, J. C. Garreau, B. Grémaud, and D. Delande, “Observation of the Anderson metal-insulator transition with atomic matter waves: Theory and experiment,” *Phys. Rev. A* **80**, 043626 (2009).
- [21] See Supplemental Material at [URL will be inserted by publisher], which includes Refs. [35–37], for details on the mapping of the  $n$ -frequency kicked rotor onto a  $n$ -dimensional Anderson model.
- [22] J. Chabé, G. Lemarié, B. Grémaud, D. Delande, P. Sriftgiser, and J. C. Garreau, “Experimental Observation of the Anderson Metal-Insulator Transition with Atomic Matter Waves,” *Phys. Rev. Lett.* **101**, 255702 (2008).
- [23] M. Lopez, J.-F. Clément, P. Sriftgiser, J. C. Garreau, and D. Delande, “Experimental Test of Universality of the Anderson Transition,” *Phys. Rev. Lett.* **108**, 095701 (2012).
- [24] See Supplemental Material at [URL will be inserted by publisher], which includes Refs. [35–37], for details on the new standing wave setup.
- [25] The center of the momentum distribution is convoluted with the initial distribution, that is why it is excluded from the fits.
- [26] At longer times, of the order of 1000 kicks, small deviations from the exponential profile are visible. They are due to residual decoherence processes. We estimate the coherence time to be of the order of 400 kicks, a significant improvement with respect to our previous setup.
- [27] B. V. Chirikov, “A universal instability of many-dimensional oscillator systems,” *Phys. Rep.* **52**, 263–379 (1979).
- [28] We have also estimated directly the average kinetic energy from the full momentum distribution and find similar results. The error bars are however larger because of the difficulty to measure accurately the tails of the distribution which contribute significantly to  $\langle p^2 \rangle$ .
- [29] G. Lemarié, D. Delande, J. C. Garreau, and P. Sriftgiser, “Classical diffusive dynamics for the quasiperiodic

kicked rotor,” J. Mod. Opt. **57**, 1922–1927 (2010).

[30] J. Kroha, T. Kopp, and P. Wölfle, “Self-consistent theory of Anderson localization for the tight-binding model with site-diagonal disorder,” Phys. Rev. B **41**, 888–891 (1990).

[31] I. Zambetaki, Q. Li, E. N. Economou, and C. M. Soukoulis, “Localization in Highly Anisotropic Systems,” Phys. Rev. Lett. **76**, 3614–3617 (1996).

[32] C. Tian, A. Kamenev, and A. Larkin, “Ehrenfest time in the weak dynamical localization,” Phys. Rev. B **72**, 045108 (2005).

[33] M. Lopez, J.-F. Clément, G. Lemarié, D. Delande, P. Sriftgiser, and J. C. Garreau, “Phase diagram of the anisotropic Anderson transition with the atomic kicked rotor: theory and experiment,” New J. Phys **15**, 065013 (2013).

[34] D. L. Shepelyansky, “Some statistical properties of simple classically stochastic quantum systems,” Physica D **8**, 208–222 (1983).

[35] [first reference in Supplemental Material not already in Letter] D. Vollhardt and P. Wölfle, “Self-Consistent Theory of Anderson Localization,” in *Electronic Phase Transitions*, edited by Hanke, W. and Kopaev Yu. V. (Elsevier, 1992) pp. 1–78.

[36] P. Wölfle and D. Vollhardt, “Self-Consistent Theory of Anderson Localization: General Formalism and Applications,” Int. J. Mod. Phys B **24**, 1526–1554 (2010).

[37] [last reference in Supplemental Material not already in Letter] C. Tian, A. Altland, and M. Garst, “Theory of the Anderson Transition in the Quasiperiodic Kicked Rotor,” Phys. Rev. Lett. **107**, 074101 (2011).